Jussi Salmi, Andreas Richter, and Visa Koivunen. 2007. Tracking of MIMO propagation parameters under spatio-temporal scattering model. In: Michael B. Matthews (editor). Conference Record of the 41st Asilomar Conference on Signals, Systems and Computers (ACSSC 2007). Pacific Grove, CA, USA. 4-7 November 2007, pages 666-670.

Tracking of MIMO Propagation Parameters under Spatio-Temporal Scattering Model

Jussi Salmi, Andreas Richter and Visa Koivunen
Signal Processing Laboratory/SMARAD CoE
Helsinki University of Technology
Espoo, Finland

***Abstract*— The paper presents novel, computationally efficient methods for tracking radio propagation path parameters from measured tensor-valued MIMO observations. The measurement covariance model is comprised of spatio-temporal scattering plus measurement noise, leading to a shifted Kronecker structure. We derive novel expressions to handle these large ($10^5 \times 10^5$) covariance matrices in the Extended Kalman Filter, used for tracking the dominant propagation paths. Furthermore, we introduce a method to model signals with a given angular distribution, observed with arbitrary antenna arrays. Finally, results for estimating dominant propagation paths from simulated data having an angular (von Mises-Fisher), and temporal (exponential) distributed scattering component are presented, accompanied by a real world example.**

I. Introduction

Future wireless communication systems will exploit the rich spatial and temporal diversity of the radio propagation environment. This calls for new advanced channel models, which need to be verified by real-world channel sounding measurements. In this context the reliable estimation and tracking of the model parameters from measured data is of particular interest.

In this paper, we discuss the modeling and estimation of radio propagation channels for wireless Multiple-Input-Multiple-Output (MIMO) communication systems based on channel sounding measurements. Our model consists of two components

1) Dominant propagation paths (plane waves) described by geometric and polarimetric parameters
2) The Dense Multipath Component (DMC) describing the spatio-temporal distributed diffuse scattering in the channel.

The DMC is incorporated in the channel covariance. In earlier work [3]–[6] the DMC had a structure in delay, but the spatial distribution was assumed to be uniform. In this paper we extend the DMC model to have structure in the spatial domain as well. Such extension has been discussed in [1]. In that work the authors derived a maximum likelihood estimator for a covariance model having von Mises distribution in azimuth at one link end, as well as an exponential delay profile. The analysis in [1] was also limited to simulations with linear antenna arrays. Our first contribution in this work lies in extending the spatial model to describe signals given any angular distribution in azimuth and elevation using arbitrary antenna arrays.

The research was partly funded by the WILATI project. First author would like to thank Finnish Technology Promotion Foundation (TES), Emil Aaltonen Foundation and Elektroniikkainsinöörien Säätiö (EIS) for financial support.

The measurement covariance matrices in channel sounding are, in general, very large. Therefore we propose to approximate the covariance matrices with a Kronecker structured matrix. This is motivated by the fact that the channel observation can be interpreted as a tensor, for which efficient computational techniques exist [2]. Our covariance model is comprised of additive white Gaussian measurement noise plus the DMC component [3], which takes the spatial correlation at Tx and Rx as well as the exponential delay profile into account. This results in a shifted Kronecker structure for the measurement covariance matrix. Our second contribution is to show the feasibility of applying these improved covariance models with the previously established Extended Kalman Filter (EKF) expressions used for propagation path parameter estimation [4], [5]. Additionally, in order to reduce the computational complexity, we present an approximation technique for expressing n-way arrays (tensors) based on Singular Value Decompositions (SVD). To evaluate the performance of the proposed techniques, we use simulations as well as real world radio channel measurements.

II. Propagation Parameter Estimation

In our previous work, we have investigated the estimation of radio channel model parameters using a two component model comprised of the sum of concentrated propagation paths and the DMC [3]. We have then formulated a state-space model for tracking these parameters using an EKF [4]–[6]. The first model component, i.e. the concentrated propagation paths, are described with L number of parameters (L depending on the measurement setup, typically $L \approx 10$) such as Time Delay of Arrival (TDoA) τ, Direction of Arrival (DoA) φ_R, ϑ_R and Direction of Departure (DoD) φ_T, ϑ_T as well as polarization weights γ. These parameters are illustrated in Fig. 1(a). The total number (LP) of parameters to estimate for the propagation paths depends on the number of paths P (typically $P \approx 10 - 100$). A histogram for the number of tracked paths $\hat{P}$ in a measurement campaign of over 27000 snapshots is shown in Fig. 1(b).

The second component in our model, the DMC, describes the diffuse scattering in the radio channel, and is modeled as a stochastic circular-complex Gaussian distributed process

978-1-4244-2110-7/08/$25.00 ©2007 IEEE

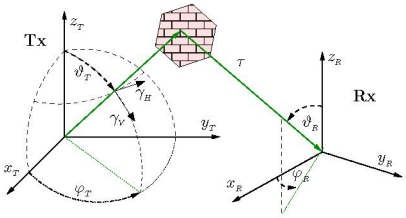

(a) Propagation path parameters.

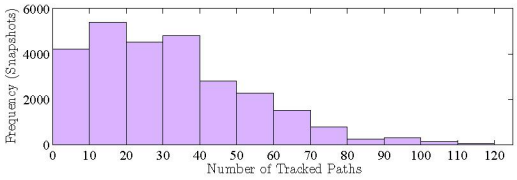

(b) Histogram of tracked paths $\hat{P}$.

Fig. 1. Illustration of the propagation path parameters as well as the histogram of the number of tracked paths.

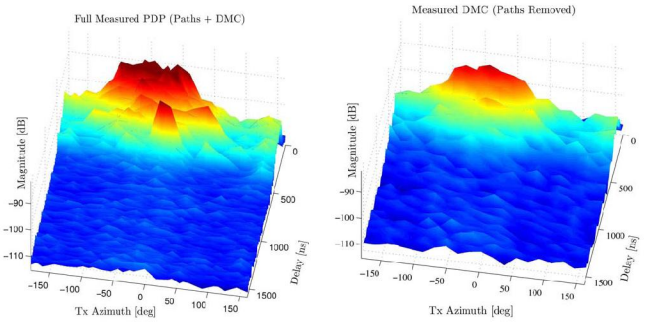

(a) All data averaged over Rx channels.

(b) Same as Fig. 2(a) with dominant propagation paths removed.

Fig. 2. Instantaneous Power-Delay-Direction-Profile from a MIMO measurement with 16 element circular array in a street scenario.

with specific correlation properties. Using a stochastic model for the DMC has several advantages. First of all, partly due to measurement system limitations, it is impossible to estimate all the necessary information for all observed diffuse scattering in a radio channel by using the discrete propagation path model. Thus DMC provides a better fitting measurement model. Another obvious gain is in the model complexity, since only a few parameters need to be estimated to characterize the underlying stochastic process.

So far we have developed an estimation procedure [4]–[6] based on a simplifying assumption of the DMC being angular-white, i.e., the diffuse scattered signal components arrive uniformly from all directions, having an exponentially decaying delay profile. Based on the analysis of many different channel sounding measurements it has turned out that the assumption of angular-white DMC does not necessarily hold. In particular, it has been observed that this assumption is violated in e.g. street canyon scenarios. Besides the incomplete channel description, this modeling error also leads to deteriorated propagation path parameter estimates, which rely on the estimates of the unknown DMC parameters. Especially detection of new paths as well as path quality assessment suffer from the inadequate DMC model. Fig. 2 illustrates a street canyon measurement conducted in downtown Ilmenau, Germany (setup described in [7]). These 3-D Power-Delay-Direction Profiles have been estimated using beamforming at the transmitter (Tx) end for a 16-element circular array. After removing the dominant propagation paths from the measured data (Fig. 2(a), using about $P = 50$ high resolution estimates for propagation paths in this case), the resulting residual (Fig. 2(b)) clearly reveals that the remaining scattering component has a non-uniform spatial distribution.

III. State-space Model

The state-space model used in this paper includes the state equation, describing the dynamic behavior of propagation path parameters $\boldsymbol{\theta} \in \mathbb{R}^{LP}$, and the measurement equation, with nonlinear mapping $\mathbf{s}(\boldsymbol{\theta})$ of the double-directional propagation model [8] parameters to the channel sounder output data.

For a full channel sounding measurement setup[1], the state vector is defined as

$$\boldsymbol{\theta}_k = [\ \underbrace{\boldsymbol{\mu}^{\mathrm{T}}}_{5P\times 1}\ \underbrace{\Delta\boldsymbol{\mu}^{\mathrm{T}}}_{5P\times 1}\ \underbrace{\boldsymbol{\alpha}^{\mathrm{T}}}_{4P\times 1}\ \underbrace{\boldsymbol{\phi}^{\mathrm{T}}}_{4P\times 1}\ \underbrace{\Delta\overline{\phi}^{\mathrm{T}}}_{P\times 1}\ ]^{\mathrm{T}}, \tag{1}$$

where $\boldsymbol{\mu}$ are the structural path parameters (delays, angles), $\Delta\boldsymbol{\mu}$ being their rate of change, $\boldsymbol{\alpha}$ contains the logarithms of the polarimetric path weight magnitudes, $\boldsymbol{\phi}$ are the path weight phases, and $\Delta\overline{\phi}$ are the short time mean of the phase changes (also related to the Doppler shift). This parametrization provides linear, zero-mean, and stationary state transition process, well suited for EKF implementation. The state transition is thus given by

$$\boldsymbol{\theta}_k = \boldsymbol{\Phi}_k\boldsymbol{\theta}_{k-1} + \mathbf{v}_k,$$

where $\boldsymbol{\Phi}$ is the state transition matrix and $\mathbf{v}_k \sim \mathcal{N}(\mathbf{0}, \mathbf{Q})$ is the state noise with covariance matrix $\mathbf{Q}$.

The measurements are assumed to obey

$$\mathbf{y} \sim \mathcal{N}_C\left(\mathbf{s}(\boldsymbol{\theta}), \mathbf{R}_o(\boldsymbol{\theta}_{DMC})\right) \in \mathbb{C}^{M\times 1}, \tag{2}$$

where the noise process covariance $\mathbf{R}_o(\boldsymbol{\theta}_{DMC})$ has structure in delay as well as in angular domain. It should be noted that the dimension of a measurement is currently $M = M_f M_T M_R > 10^5 >> LP$. For example a setup with $M_f = 510$ frequency (delay) samples, $M_T = 32$ Tx ports and $M_R = 32$ Rx ports, yields $M \approx 5 \cdot 10^5$ complex samples per observation. Thus any approach involving the use of the full $10^5 \times 10^5$ covariance matrix is clearly infeasible with current computational resources.

IV. Algorithms

A. EKF Expressed in terms of Score function and FIM

The high level description of the algorithm is sketched in Fig. 3. The EKF uses Taylor series expansion for linearizing the state-space model. The EKF equations for the filtering

[1]The term *full* refers here to a setup able to capture both azimuth and elevation, as well as dual polarization at both link ends.

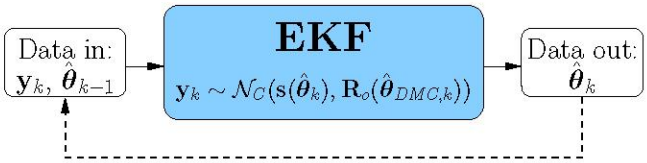

Fig. 3. High level description of the propagation path estimation method.

error covariance $\mathbf{P}_{(k|k)}$ and the filtered state $\boldsymbol{\theta}_{(k|k)}$ can be expressed in terms of the Score function

$$\begin{aligned}\mathbf{q}(\mathbf{y}|\boldsymbol{\theta},\mathbf{R}) &= \frac{\partial}{\partial\boldsymbol{\theta}}\mathcal{L}(\mathbf{y}|\boldsymbol{\theta},\mathbf{R}) \\ &= 2\cdot\Re\left\{\mathbf{D}^{\mathrm{H}}(\boldsymbol{\theta})\mathbf{R}^{-1}\tilde{\mathbf{y}}\right\}, \end{aligned} \tag{3}$$

where

$$\tilde{\mathbf{y}} = \mathbf{y} - \mathbf{s}(\boldsymbol{\theta}), \tag{4}$$

and the Fisher Information Matrix (FIM)

$$\begin{aligned}\mathbf{J}(\boldsymbol{\theta},\mathbf{R}) &= -\mathrm{E}\left\{\frac{\partial}{\partial\boldsymbol{\theta}}\mathcal{L}(\mathbf{y}|\boldsymbol{\theta},\mathbf{R})\left(\frac{\partial}{\partial\boldsymbol{\theta}}\mathcal{L}(\mathbf{y}|\boldsymbol{\theta},\mathbf{R})\right)^{\mathrm{T}}\right\} \\ &= 2\cdot\Re\left\{\mathbf{D}^{\mathrm{H}}(\boldsymbol{\theta})\mathbf{R}^{-1}\mathbf{D}(\boldsymbol{\theta})\right\}. \end{aligned} \tag{5}$$

Expression $\mathcal{L}(\mathbf{y}|\boldsymbol{\theta},\mathbf{R})$ denotes the log-likelihood function of (2), and $\mathbf{D} \in \mathbb{C}^{M\times LP}$ is the Jacobian matrix (first order partial derivatives $\frac{\partial}{\partial\boldsymbol{\theta}}\mathbf{s}(\boldsymbol{\theta})$). Applying (3) and (5) to the EKF equations yields

$$\mathbf{P}_{(k|k)} = \left(\mathbf{P}^{-1}_{(k|k-1)} + \mathbf{J}(\hat{\boldsymbol{\theta}}_{(k|k-1)},\mathbf{R}_k)\right)^{-1} \tag{6}$$

$$\hat{\boldsymbol{\theta}}_{(k|k)} = \hat{\boldsymbol{\theta}}_{(k|k-1)} + \underbrace{\mathbf{P}_{(k|k)}\mathbf{q}\left(\mathbf{y}_k|\hat{\boldsymbol{\theta}}_{(k|k-1)},\mathbf{R}_k\right)}_{\triangle\boldsymbol{\theta}_k}. \tag{7}$$

One should note that the straightforward computation of (3) and (5) involves huge matrices $\mathbf{D} \in \mathbb{C}^{M\times LP}$ and $\mathbf{R}^{-1} \in \mathbb{C}^{M\times M}$ and is thus infeasible.

B. Covariance Model vs. Computational Complexity

In the following discussion on computational complexity (number of additions and multiplications) we assume the system dimensions according to Table I.

1) Full Kronecker Structure: Computationally feasible and efficient solutions for (3) and (5) were presented in [3]. There, the assumption was that the full covariance matrix of the measured radio channel $\mathbf{R}_H$ is structured as

$$\mathbf{R}_H = \mathbf{R}_R \otimes \mathbf{R}_T \otimes \mathbf{R}_f \in \mathbb{C}^{M\times M}. \tag{8}$$

TABLE I
SYSTEM DIMENSIONS IN THE COMPLEXITY EXAMPLES.

M_f	M_T	M_R	L	P
193	16	16	13	40

Then (3) and (5) could be expressed as[2]

$$\mathbf{q}_H = 2\Re\left\{\left(\mathbf{R}_R^{-1}\mathbf{D}_R\Diamond\mathbf{R}_T^{-1}\mathbf{D}_T\Diamond\mathbf{R}_f^{-1}\mathbf{D}_f\right)^{\mathrm{H}}\tilde{\mathbf{y}}\right\}, \tag{9}$$

$$\mathbf{J}_H = 2\Re\left\{\mathbf{D}_R^{\mathrm{H}}\mathbf{R}_R^{-1}\mathbf{D}_R \odot \mathbf{D}_T^{\mathrm{H}}\mathbf{R}_T^{-1}\mathbf{D}_T \odot \mathbf{D}_f^{\mathrm{H}}\mathbf{R}_f^{-1}\mathbf{D}_f\right\}, \tag{10}$$

where $\mathbf{D} = \mathbf{D}_R\Diamond\mathbf{D}_T\Diamond\mathbf{D}_f$. Utilizing a known solution [3] for memory efficient computation of expressions of type $(\mathbf{A}_3\Diamond\mathbf{A}_2\Diamond\mathbf{A}_1)^{\mathrm{H}}\mathbf{x}$ in (9), it can be concluded that the expressions (9) and (10) involve matrices, whose size are only $M_i \times M_i$ and $M_i \times LP$, $i \in \{f,R,T\}$ with $M_i \ll M$. The computational complexities (multiplications + additions) are $\mathcal{O}\left(2(LP)\sum_i M_i^2 + 7(LP)\prod_i M_i\right) \approx \mathcal{O}\left(10^8\right)$ for (9), and $\mathcal{O}\left(2(LP)\sum_i M_i^2 + 2(LP)^2\sum_i M_i\right) \approx \mathcal{O}\left(10^8\right)$ for (10).

2) Shifted Kronecker Structure: The model (8) assumes that the angular (Tx and Rx) and delay domains in the measured data tensor are uncoupled (suggested also e.g. in [9], [10]). However, the model (8) is not adequate for our purposes, since it does not take the measurement noise into account. We model the measurement noise as an additive white circular complex Gaussian process with variance σ^2, yielding

$$\mathbf{R}_o = \mathbf{R}_R \otimes \mathbf{R}_T \otimes \mathbf{R}_f + \sigma^2\mathbf{I}_M. \tag{11}$$

The additive term $\sigma^2\mathbf{I}_M$ destroys the Kronecker structure of $\mathbf{R}_H$ in (8), and the expressions (9) and (10) used in [3] for computing products involving $\mathbf{R}_o$ are no longer applicable. In previous work [4]–[6], the Kronecker structure was recovered by making some very limiting assumptions, namely $\mathbf{R}_R = \mathbf{I}_R$ and $\mathbf{R}_T = \mathbf{I}_T$, yielding

$$\mathbf{R}_I = \mathbf{I}_R \otimes \mathbf{I}_T \otimes \left(\mathbf{R}_f + \sigma^2\mathbf{I}_f\right). \tag{12}$$

This allowed the use of, and even simplified, the expressions (9) and (10) with the expence of modeling error.

C. Solutions for the Score and the FIM with Shifted Kronecker Structured Measurement Covariance

In the following, we consider the most general of the presented approaches, i.e., the shifted Kronecker structure $\mathbf{R}_o$ (11), and present computationally feasible expressions to solve the Score function (3) and the FIM (5).

The matrix $\mathbf{R}_o$ can be expressed using the eigenvalue decomposition of (11) as

$$\begin{aligned}\mathbf{R}_o &= \mathbf{U}\boldsymbol{\Lambda}\mathbf{U}^{\mathrm{H}} + \sigma^2\mathbf{I}_M \\ &= (\mathbf{U}_R\otimes\mathbf{U}_T\otimes\mathbf{U}_f)(\boldsymbol{\Lambda}_R\otimes\boldsymbol{\Lambda}_T\otimes\boldsymbol{\Lambda}_f + \sigma^2\mathbf{I}_M)\cdot \\ &\quad (\mathbf{U}_R\otimes\mathbf{U}_T\otimes\mathbf{U}_f)^{\mathrm{H}}. \end{aligned} \tag{13}$$

This allows us to formulate the Score function as

$$\mathbf{q}_o = 2\Re\left\{\left(\mathbf{D}'_R\Diamond\mathbf{D}'_T\Diamond\mathbf{D}'_f\right)^{\mathrm{H}}\left(\boldsymbol{\Lambda}_o^{-1}\tilde{\mathbf{y}}_{\mathrm{U}}\right)\right\}, \tag{14}$$

where

$$\mathbf{D}'_i = \mathbf{U}_i^{\mathrm{H}}\mathbf{D}_i,\ i \in \{f,T,R\}, \tag{15}$$

$$\boldsymbol{\Lambda}_o = (\boldsymbol{\Lambda}_R\otimes\boldsymbol{\Lambda}_T\otimes\boldsymbol{\Lambda}_f + \sigma^2\mathbf{I}_M), \tag{16}$$

[2]The operator $\Diamond$ denotes the Khatri-Rao product, i.e., column-wise Kronecker product and the operator $\odot$ denotes the Schur product, i.e., element-wise product of matrices.

and $\tilde{\mathbf{y}}_{\mathrm{U}}$ is a vector having the matrices of eigenvectors $\mathbf{U}_i$ multiplied dimension-wise with $\tilde{\mathbf{y}}$ (4). The complexity and matrix dimensions of (14) are similar to those of (9).

The expression of the FIM (5), on the other hand, involves additional operations. The FIM using $\mathbf{R}_o$ (13) can be expressed as

$$\mathbf{J}_o = 2\Re\left\{ \left(\mathbf{D}'_R \Diamond \mathbf{D}'_T \Diamond \mathbf{D}'_f\right)^{\mathrm{H}} \mathbf{\Lambda}_o^{-1} \left(\mathbf{D}'_R \Diamond \mathbf{D}'_T \Diamond \mathbf{D}'_f\right) \right\}. \quad (17)$$

The inverse of the diagonal matrix $\mathbf{\Lambda}_o$ (16) in (17) cannot be factorized to a Kronecker product, and thus the form (10) is not applicable, whereas the straightforward computation is infeasible due to huge matrix dimensions. A feasible solution for (17) can be expressed as

$$\mathbf{J}_o = \sum_{m_f=1}^{M_f} \sum_{m_R=1}^{M_R} \sum_{m_T=1}^{M_T} \Big[\frac{1}{\lambda_{f,m_f} \lambda_{T,m_T} \lambda_{R,m_R} + \sigma^2} \cdot \left(\mathbf{d}'^{\mathrm{H}}_{f,m_f} \mathbf{d}'_{f,m_f} \odot \mathbf{d}'^{\mathrm{H}}_{T,m_T} \mathbf{d}'_{T,m_T} \odot \mathbf{d}'^{\mathrm{H}}_{R,m_R} \mathbf{d}'_{R,m_R}\right) \Big], \quad (18)$$

where λ_{i,m_i} are the m_i^{th} singular values on the individual diagonal matrices $\mathbf{\Lambda}_i$ in (16), and $\mathbf{d}'_{i,m_i}$ are the m_i^{th} *row vectors* of the matrices $\mathbf{D}'_i$ in (17). The expression (18) includes only outer products of LP-length and Schur products of matrices with size $LP \times LP$. The complexity after taking f and T related common terms out of the sums is still very high, namely $\mathcal{O}\left((LP)^2 \prod_i M_i\right) \approx \mathcal{O}\left(10^{10}\right)$.

D. SVD based Tensor Approximation of the FIM

To reduce the complexity of (18), or dimensions in (17), we introduce a method, which is essentially a Singular Value Decomposition (SVD) based approximation of a tensor [2].

Let us form a 3-D tensor $\mathcal{K}_{f,T,R} \in \mathbb{R}^{M_f \times M_T \times M_R}$, consisting of the diagonal elements of $\mathbf{\Lambda}_o^{-1}$ (16). The tensor $\mathcal{K}_{f,T,R}$ is reshaped into a matrix $\mathbf{K}_{f,TR} \in \mathbb{R}^{M_f \times M_T M_R}$, whose SVD is given by

$$\mathbf{K}_{f,TR} = \mathbf{U}_f \mathbf{\Xi}_{f,TR} \mathbf{V}^{\mathrm{H}}_{TR}. \quad (19)$$

For each $m'_f = \{1 \ldots M'_f\}$ highest singular values $\boldsymbol{\xi}_{f,TR}(m'_f)$ in $\mathbf{\Xi}_{f,TR}$ we reshape the m'^{th}_f column of $\mathbf{V}_{TR}$ to form a matrix $\mathbf{K}_{T,R}(m'_f) \in \mathbb{R}^{M_T \times M_R}$ and compute its SVD as

$$\mathbf{K}_{T,R}(m'_f) = \mathbf{U}_T(m'_f) \mathbf{\Xi}_{T,R}(m'_f) \mathbf{V}_R(m'_f)^{\mathrm{H}}. \quad (20)$$

Now $m'_T = \{1 \ldots M'_T\}$ largest singular values $\xi_{T,R}(m'_f, m'_T)$ in $\mathbf{\Xi}_{T,R}(m'_f)$ for each m'_f are selected to form an approximation of the FIM as

$$\mathbf{J}_a(\boldsymbol{\theta}, \mathbf{R}_o) = \sum_{m'_f}^{M'_f} \Bigg\{ \left(\mathbf{D}'^{\mathrm{H}}_f \tilde{\mathbf{\Lambda}}_f(m'_f) \mathbf{D}'_f\right) \odot \sum_{m'_T}^{M'_T} \Big\{ \left(\mathbf{D}'^{\mathrm{H}}_T \tilde{\mathbf{\Lambda}}_T(m'_f, m'_T) \mathbf{D}'_T\right) \odot \left(\mathbf{D}'^{\mathrm{H}}_R \tilde{\mathbf{\Lambda}}_R(m'_f, m'_T) \mathbf{D}'_R\right) \Big\} \Bigg\}. \quad (21)$$

The diagonal matrices $\tilde{\mathbf{\Lambda}}_i$ in (21) are defined as

$$\tilde{\mathbf{\Lambda}}_f(m'_f) = \mathrm{diag}\left\{\mathbf{u}_f(m'_f) \xi_{f,TR}(m'_f)\right\},$$
$$\tilde{\mathbf{\Lambda}}_T(m'_f, m'_T) = \mathrm{diag}\left\{\mathbf{u}_T(m'_f, m'_T) \xi_{T,R}(m'_f, m'_T)\right\},$$
$$\tilde{\mathbf{\Lambda}}_R(m'_f, m'_T) = \mathrm{diag}\left\{\mathbf{v}_R(m'_f, m'_T)\right\},$$

where $\mathbf{u}_j(m'_i)$ denotes the m'^{th}_i column of matrix $\mathbf{U}_j$. This solution has computational complexity

$$\mathcal{O}\left((LP)^2 M'_f (2M'_T(M_T + M_R) + M_f)\right) \approx \mathcal{O}\left(10^9\right), \quad (22)$$

assuming $M'_f = 12 << M_f$ and $M'_T = 5 << M_T$ based on the analysis in Section V-B.

V. Results

A. DMC Modeling

To simulate spatially distributed scattering, we introduce a method to map an angular power distribution to a real world antenna array output. The model for simulating the antenna array can be expressed as

$$\mathbf{R}_a = \mathbf{G}_a \mathbf{A}_{\varphi_s,\vartheta_s} \mathbf{K}_{\varphi_s,\vartheta_s} \mathbf{A}^{\mathrm{H}}_{\varphi_s,\vartheta_s} \mathbf{G}^{\mathrm{H}}_a \in \mathbb{C}^{M_a \times M_a}, \quad (23)$$

where the subindex $a \in [T, R]$ denotes either transmitter or receiver, respectively. The matrix $\mathbf{G}_a \in \mathbb{C}^{M_a \times N_\varphi N_\vartheta}$ denotes the Effective Aperture Distribution Function (EADF) [11]. EADF is a *mode* domain expression obtained from an antenna array calibration through a two-dimensional Fourier-transformation, and it defines the array response for a given signal direction. The matrix $\mathbf{A}_{\varphi_s,\vartheta_s} \in \mathbb{C}^{N_\varphi N_\vartheta \times N_s}$ is the Fourier transformation from *angular* domain to *mode* domain, and $\mathbf{K}(\boldsymbol{\varphi}_s, \boldsymbol{\vartheta}_s) \in \mathbb{R}^{N_s \times N_S}$ denotes an approximation of the angular domain covariance for N_s sampling points $(\boldsymbol{\varphi}_s, \boldsymbol{\vartheta}_s)$ on a sphere. Initially, we select a diagonal matrix having the angular pdf values evaluated at the sampling points.

As an initial approach we use the von Mises-Fisher angular distribution [12] to model the diffuse scattering in the angular domain. Fig. 4(a) shows the Power-Delay Profile (PDP) of the residual in Fig. 2(b) averaged over all Tx-Rx channels. Also two simulated PDPs are shown. The first simulation (Approach #1) is using angular-white DMC (12), and the proposed Approach #2 (11) uses the von Mises-Fisher angular distribution. Both fit well to the measured PDP in the delay domain in Fig. 4(a), but Fig. 4(b) reveals the difference in the angular domain. The von Mises-Fisher distributed model in (Approach #2) is very similar to the measured one, whereas the assumption on angular-whiteness (Approach #1) is clearly not valid.

B. Evaluation of the SVD Tensor Approximation

The performance of the SVD based tensor approximation (21) is analyzed by running the EKF on measurement data, using different thresholds ϵ_f for selecting how many components M'_f and M'_T are used for evaluating (21). The thresholds are defined as

$$\frac{\xi_{f,TR}(M'_f)}{\xi_{f,TR}(1)} > \epsilon_f > \frac{\xi_{f,TR}(M'_f + 1)}{\xi_{f,TR}(1)}, \quad (24)$$

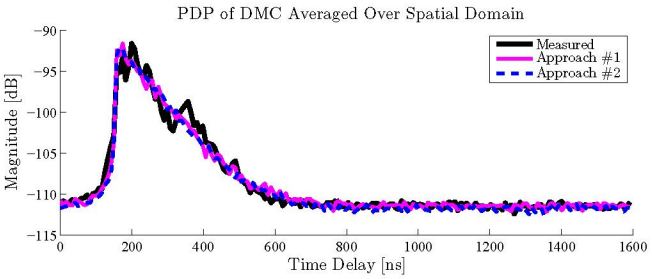

(a) PDP of DMC in the delay domain (averaged over Rx and Tx channels).

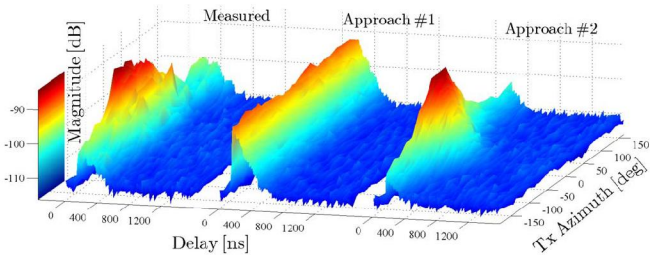

(b) Spatial PDP of DMC.

Fig. 4. Illustration of different approaches to model DMC. In the delay domain (Fig. 4(a)) both approaches #1 and #2 fit well to the measured DMC. In the angular domain (Fig. 4(b)) Approach #1 clearly fails to match the measured DMC, whereas the proposed angular distribution (Approach #2) fits well to the real world equivalent.

and

$$\frac{\xi_{T,R}(m'_f, M'_T)}{\xi_{T,R}(m'_f, 1)} > \epsilon_T(m'_f) > \frac{\xi_{T,R}(m'_f, M'_T + 1)}{\xi_{T,R}(m'_f, 1)}, \quad (25)$$

where $\epsilon_T(m'_f) = \frac{\xi_{T,R}(1)}{\xi_{T,R}(m'_f)}\epsilon_f$. Thus, setting $\epsilon_f = 0$ provides the exact solution, i.e. $M'_f = M_f$ and $M'_T = M_T$.

Let us define two error criteria:

1) The approximation error is propagated to the filtering update $\Delta\boldsymbol{\theta}_k$ of the EKF in (7), and compared with the estimated filtering error variance $\hat{\boldsymbol{\sigma}}^2_{(k|k)} = \text{diag}\{\mathbf{P}_{(k|k)}\}$ (6), yielding a relative RMSE of N samples

$$e_1(\epsilon_f) = \sqrt{\frac{1}{N}\left(|\Delta\boldsymbol{\theta}_k - \Delta\hat{\boldsymbol{\theta}}_k(\epsilon_f)|^2\right)^{\mathrm{T}} \hat{\boldsymbol{\sigma}}^{-2}_{(k|k)}}. \quad (26)$$

2) The second error criterion is the one used in e.g. [10], given by

$$e_2(\epsilon_f) = \sqrt{\frac{1}{N}\sum_{n=1}^{N} \frac{||\mathbf{R}_o - \hat{\mathbf{R}}_n(\epsilon_f)||_F}{||\mathbf{R}_o||_F}}. \quad (27)$$

The results are listed in Table II for the full decomposition $\epsilon_f = 0$, and approximations using three different thresholds. Also the average run time in Matlab for evaluating (21), the average number of modes M'_f and M'_T, and the complexity (22) are listed. Table II indicates that choosing $\epsilon_f = 10^{-6}$ gives a good trade-off with the update error being on average only 0.4% of the filtering error, and the measurement time being 1/3 of the (in practice exact[3]) solution with $\epsilon_f = 10^{-12}$.

[3]Error $e_1^2(\epsilon_f = 10^{-12})$ in Table II is in the order of IEEE double precision.

TABLE II

ANALYSIS RESULTS OF SVD BASED APPROXIMATION (SAME DIMENSIONS AS IN TABLE I, EXCEPT HERE $P \approx 53$ PATHS ON AVERAGE).

ϵ_f	e_1	e_2	Time (s)	M'_f	M'_T	Eq. (22)
0	0	0	134	193	16	$6.3 \cdot 10^{-10}$
10^{-12}	$6 \cdot 10^{-9}$	10^{-6}	12	24	10	$5.4 \cdot 10^{-9}$
10^{-6}	$4 \cdot 10^{-3}$	10^{-3}	4.0	12	5	$1.7 \cdot 10^{-9}$
10^{-2}	$4 \cdot 10^{2}$	0.1	0.9	3	2	$2.6 \cdot 10^{-8}$

All approximations give at least one decade improvement on the computation time compared to the exact solution.

VI. CONCLUSIONS

In this paper we consider the tracking of the MIMO propagation model parameters. We introduced a novel approach to model the DMC with the shifted Kronecker structured measurement covariance model allowing arbitrary angular and delay distributions. We present a method for approximating the large tensor-valued measurement covariance, yielding significant computational savings in the FIM, without loss of performance in terms of estimation error. Evaluating the approximation error of the covariance matrices by propagating the error to the parameter update step gives insight on choosing a proper threshold for approximation order adjustment.

REFERENCES

[1] C. Ribeiro, E. Ollila, and V. Koivunen, "Stochastic maximum-likelihood method for MIMO propagation parameter estimation," *IEEE Trans. Signal Processing*, vol. 55, no. 1, pp. 46–55, Jan 2007.

[2] M. E. Kilmer and C. D. M. Martin, "Decomposing a tensor," *SIAM News*, vol. 37, no. 9, Nov. 2004.

[3] A. Richter, "Estimation of radio channel parameters: Models and algorithms," Ph. D. dissertation, Technischen Universität Ilmenau, Germany, May 2005, [Online]: www.db-thueringen.de.

[4] J. Salmi, A. Richter, and V. Koivunen, "State-space modeling and propagation parameter tracking: Multitarget tracking based approach," in *Proc Asilomar Conference on Signals, Systems, and Computers*, Pacific Grove, CA, Oct. 2006, pp. 941–945.

[5] ——, "Enhanced tracking of radio propagation path parameters using state-space modeling," in *Proc. EUSIPCO 06*, Florence, Italy, September 2006.

[6] A. Richter, J. Salmi, and V. Koivunen, "An algorithm for estimation and tracking of distributed diffuse scattering in mobile radio channels," in *Signal Processing Advances in Wireless Communications*, Cannes, France, July 2006.

[7] ——, "On distributed scattering in radio channels and its contribution to mimo channel capacity," in *Proc 1st European Conference on Antennas and Propagation*, Nice, France, Nov. 2006.

[8] M. Steinbauer, A. Molisch, and E. Bonek, "The double-directional radio channel," *IEEE Antennas and Propagation Magazine*, vol. 43, no. 4, pp. 51–63, Aug. 2001.

[9] Q. H. Spencer, B. D. Jeffs, M. A. Jensen, and A. L. Swindlehurst, "Modeling the statistical time and angle of arrival characteristics of an indoor multipath channel," *IEEE Journal on Selected Areas In Communications*, vol. 18, no. 3, pp. 347–360, March 2000.

[10] K. Werner, M. Jansson, and P. Stoica, "Kronecker structured covariance matrix estimation," in *Proc IEEE ICASSP*, Honolulu, Hawai'i, USA, Apr. 2007.

[11] T. Kaiser, A. Bourdoux, H. Boche, J. R. Fonollosa, J. B. Andersen, and W. Utschick, Eds., *Smart Antennas—State of the Art*. New York, NY: Hindawi Publishing Corporation, 2005.

[12] K. V. Mardia, *Statistics of Directional Data*. Academic Press, London, UK, 1972.